Oxidation of Water to Dioxygen by Intrazeolitic $Ru(bpy)_3^{3+}$

Michael Ledney and Prabir K. Dutta*

Contribution from the Department of Chemistry, The Ohio State University, 120 West 18th Avenue, Columbus, Ohio 43210

Received December 9, 1994[⊗]

Abstract: Oxidation of water to dioxygen by $Ru(bpy)_3^{3+}$ entrapped within the supercages of zeolite Y is the object of this study. The encapsulation and isolation of individual $Ru(bpy)_3^{3+}$ molecules precludes multi-metal centered degradation reactions, typically observed in solution. With the help of diffuse reflectance, resonance Raman, and electron paramagnetic resonance spectroscopies, the mechanism of the reaction has been investigated. The proposed mechanism involves reaction of $Ru(bpy)_3^{3+}$ with water to form a covalent hydrate $Ru^{3+}(bpy)_2(bpy-H_2O)$ which is deprotonated in the presence of base to form $Ru^{3+}(bpy)_2(bpy-OH^-)$. Intramolecular electron transfer leads to the formation of a hydroxylated bipyridine radical and the metal is reduced to Ru(II). The slow step is the dissociation of this complex to form $Ru(bpy)_3^{2+}$ and hydroxyl radical ($OH^•$), which reacts with unreacted $Ru(bpy)_3^{3+}$. Hydrogen peroxide is proposed to be formed in a two-electron transfer step by reaction of hydroxide ion (OH^-) with $Ru^{3+}(bpy)_2(bpy-OH^•)$. The formation of O_2 by reaction of H_2O_2 with unreacted Ru(III) is proposed to follow similar one-electron steps as in solution. Dioxygen formation occurs almost quantitatively when the $Ru(bpy)_3^{3+}$–zeolite Y is in contact with basic solution at pH 12, whereas no formation of dioxygen is observed upon exposure to pH 4 solution. The isolation of reactive molecules in zeolite cages allows for a convenient way to study their chemistry and leads to observation of chemical pathways that do not occur in solution.

Aqueous reduction of the trivalent tris (2,2′-bipyridyl) complexes of iron, ruthenium, and osmium has been the subject of extensive research, due primarily to the capability of these complexes to oxidize water to O_2.[1] The ruthenium complex is particularly interesting because it represents the oxidative portion of the popular $Ru(bpy)_3^{2+}$-sensitized photosystem.[2] A variety of photochemical schemes for splitting H_2O to H_2 and O_2 have been proposed using this sensitizer.[2] Success of such schemes is limited by two factors. First, the oxidative quenching of the $Ru(bpy)_3^{2+}$ excited state is usually followed by a back electron transfer reaction[2a] which results in only short-lived charge separation. Second, the aqueous chemistry of $Ru(bpy)_3^{3+}$ is dominated by multimolecular decomposition processes which result in ligand degradation and CO_2 evolution.[1b,e,f] In the absence of a transition metal catalyst, the four-electron oxidation of water to dioxygen has not been observed.[1b]

The energy wasting back electron transfer reaction can be controlled by placing the reactants in a variety of heterogeneous media.[3] Several recent reports indicate that the long-range order and molecular dimensions of the cages inside zeolites make these crystalline aluminosilicates particularly attractive hosts for a variety of photochemical reactions.[4] Charge separation lifetimes ranging from picoseconds to milliseconds have been observed for organic charge transfer pairs,[4b] while reduced viologens can be generated with long lifetimes when $Ru(bpy)_3^{2+}$ is trapped in zeolite-Y and photolyzed in the presence of these electron acceptors.[4a] In these cases, the cage architecture of the zeolite allows for a specific arrangement and orientation of the molecules in space.

In this study, we exploit the cage architecture of the zeolite to isolate the highly reactive $Ru(bpy)_3^{3+}$ complex and follow its reaction with water. The solution chemistry of $Ru(bpy)_3^{3+}$ is dominated by multimolecular degradation processes.[1] A previous study[1f] using high loadings (1 per 2 supercages) of $Ru(bpy)_3^{3+}$ in zeolite resulted in chemistry that paralleled that of free solution. Encapsulation of $Ru(bpy)_3^{3+}$ in the supercages of zeolite-Y at low loadings (1 complex per 15 supercages) eliminates multimolecular processes, forcing the direct reaction of the metal complex with water. We find in the zeolite a slow oxidation of water to O_2, mediated by $Ru(bpy)_3^{3+}$. The slow kinetics of this system allow observation of several intermediates by diffuse reflectance and EPR spectroscopies, including; $OH^•$, $O_2^{•-}$, $Ru^{3+}(bpy)_2(bpy-H_2O)$, $Ru^{3+}(bpy)_2(bpy-OH^-)$, and $Ru^{2+}(bpy)_2(bpy-OH^•)$. A pH dependent mechanism which accounts for the formation of these intermediates and their kinetic behavior is proposed. To the best of our knowledge, this represents the first "uncatalyzed" oxidation of water to dioxygen by a metal tris(bipyridyl) complex.

Experimental Section

Materials. Zeolite-Y. The zeolite used in this study was purchased from Linde (lot No. 968087061020-S-1) and purified by ion exchange and calcination.

$Ru(bpy)_3^{2+}$–Y. The divalent ruthenium complex was synthesized by an extension of the method described originally by Lunsford and

[⊗] Abstract published in *Advance ACS Abstracts*, July 1, 1995.

(1) (a) Creutz, C.; Sutin, *N. Proc. Natl. Acad. Sci. U.S.A.* **1975**, *72*, 2858. (b) Ghosh, P. K.; Brunschwig, B. S.; Chou, M.; Creutz, C.; Sutin, N. *J. Am. Chem. Soc.* **1984**, *106*, 4772. (c) Lay, P. A.; Sasse, W. H. F. *Inorg. Chem.* **1985**, *24*, 4707. (d) Nord, G.; Pedersen, B.; Bjergbakke, E. *J. Am. Chem. Soc.* **1983**, *105*, 1913. (e) Serpone, N.; Boletta, F. *Inorg. Chim. Acta* **1983**, *75*, 189. (f) Quayle, W. H.; Lunsford, J. H. *Inorg. Chem.* **1982**, *21*, 97. (g) Sagüés, J. A. A.; Gillard, R. D.; Lancashire, R. J.; Williams, P. A. *J. Chem. Soc., Dalton Trans.* **1979**, 193.

(2) (a) Kalyansundaram, K. *Coord. Chem. Rev.* **1982**, *46*, 159. (b) Demas, J. N.; Crosby, G. A. *J. Am. Chem. Soc.* **1971**, *93*, 2841. (c) Borgarello, E.; Kiwi, J.; Pelizzetti, E.; Visca, M.; Gräetzel, M. *Nature* **1981**, *289*, 158. (d) Sutin, N.; Creutz, C. *Adv. Chem. Ser. 1978, No. 138*, 1. (e) Bock, C. R.; Connor, J. A.; Guiterrez, A. R.; Meyer, T. J.; Whitten, D. G.; Sullivan, B. N.; Nagel, J. K. *J. Am. Chem. Soc.* **1979**, *101*, 4815. (f) Lehn, J. M.; Sauvage, J. P.; Ziessel, R. *Nouv. J. Chim.* **1980**, *4*, 355.

(3) (a) *Photochemistry in Organized and Constrained Media*; Ramamurthy, V., Ed.; VCH: New York, 1991. (b) O'Regan, B.; Gräetzel, M.; *Nature*, **1991**, *353*, 737.

(4) (a) Borja, M.; Dutta, P. K. *Nature* **1993**, *362*, 43. (b) Yoon, K. B.; Hubig, S. M.; Kochi, J. K. *J. Phys. Chem.* **1994**, *98*, 3865. (c) Beer, R.; Binder, F.; Calzaferri, G. *J. Photochem. Photobiol. A: Chem.* **1992**, *69*, 67. (d) Mallouk, T. E.; Kim, Y. I. *J. Phys. Chem.* **1992**, *96*, 2879. (e) Blatter, F.; Frei, H. *J. Am. Chem. Soc.* **1994**, *116*, 1812.

0002-7863/95/1517-7687$09.00/0

co-workers.[5] This results in clean samples devoid of mono- or bis-(bipyridine) ruthenium complexes and excess ligand.[6a] The ruthenium loading was determined by X-ray fluorescence spectroscopy.[6c] Samples used in this study contain 31 μmol $Ru(bpy)_3^{2+}$ per gram of zeolite, or ~1 complex per 15 supercages.

$Ru(bpy)_3^{3+}$−Y. Pellets (~20 mg) of $Ru(bpy)_3^{2+}$−zeolite-Y were dehydrated for 2 h at 300 °C and 10^{-4} Torr. After being cooled to 65 °C the samples were exposed to chlorine gas (~760 Torr) for 45 min. The samples were then evacuated for 45 min to remove excess chlorine. Subsequent sample manipulations were performed in an atmosphere of dry nitrogen to avoid contamination and premature hydration.

Co^{2+}−$Ru(bpy)_3^{2+}$−Y. Cobalt(II) was introduced into $Ru(bpy)_3^{2+}$−Y samples by ion exchange from a 0.1 M $CoCl_2$ solution.

Methods. Diffuse Reflectance Spectroscopy. A Shimadzu UV 265 spectrometer equipped with a Harrick diffuse reflectance attachment was used to obtain diffuse reflectance spectra. These spectra were then Kubelka−Munk corrected[7] with a $BaSO_4$ background. $Ru(bpy)_3^{3+}$−Y pellets were hydrated with excess deionized water or with aqueous solutions adjusted to the appropriate pH with either dilute HCl or dilute NaOH. At various intervals, the excess water was removed, and a spectrum of the solid was recorded.

Resonance Raman Spectroscopy. $Ru(bpy)_3^{3+}$−Y samples were sealed in a spinning Raman cell after hydration for the specified amount of time. The 406.7-nm line of a Kr^+ ion laser (Coherent 100) was used for excitation.

Electron Paramagnetic Resonance Spectroscopy. In order to obtain good EPR spectra, the samples exposed to aqueous solutions needed to be dehydrated by a 20-min evacuation at 10^{-4} Torr to remove excess water. A Brüker ESP300 spectrometer operating in the X-band region was used. The temperature was maintained at 110 K with a liquid nitrogen steam assembly. Microwave power was typically 6.3 mW, with a resonant frequency of 9.47 GHz. Modulation was 100 kHz, with a 10-kHz modulation amplitude. Typical four scan-spectra lasted 20 min at 600 ms time constant.

Gas Chromatography. $Ru(bpy)_3^{3+}$−Y pellets were hydrated with helium-purged aqueous solutions and sealed in a septum equipped airtight reaction vessel (Supelco, 0.3 mL). The system was allowed to react for ≈24 h after which a 10 μL sample of the headspace was injected into the gas chromatograph. A Hewlett Packard Model 5890 gas chromatograph with a thermal conductivity detector was used. The column was a 3 ft × 0.25 in. molecular sieve 5A (Supelco) heated to 35 °C with helium carrier gas flowing at 60 mL/min.

Mass Spectrometry. $Ru(bpy)_3^{3+}$ pellets were hydrated with 99% $H_2{}^{18}O$ (Isotec, Inc.) and again sealed in airtight reactors under helium. After 24 h, 10 μL of the headspace gas was injected into the a Hewlett Packard 5970 MSD GC-MS. The magnitude of the peak at mass 36 was compared to that of mass 32 as a confirmation that the oxygen observed did indeed come from the water. In addition, 1 μL of the $H_2{}^{18}O$ (post reaction) was directly injected into a high-resolution mass spectrometer (VG 70-250S) and the presence of dissolved oxygen at mass 36 was examined.

Results

Formation of $Ru(bpy)_3^{3+}$. Zeolite-Y has a unit cell composition of $Na_{56}(Al_{56}Si_{136}O_{384})\cdot 235H_2O$ and is composed of 13 Å supercages accessible through four tetrahedrally arranged 7-Å windows.[8] This microstructure provides an ideal matrix for isolation of the 12.1-Å $Ru(bpy)_3^{2+}$ complex. Once synthesized within a supercage, the ruthenium complex is trapped, but it can interact with solvent in the supercage or other molecules in neighboring cages through the 7-Å windows. In effect, the zeolite functions to eliminate translational diffusion of the $Ru(bpy)_3^{2+}$, while maintaining an aqueous environment around the complex. In addition, by fixing the loading level on the order of 1 $Ru(bpy)_3^{2+}$ per 15 supercages, the immediate cages surrounding each Ru center were unoccupied. Lunsford and coworkers first reported the synthesis of $Ru(bpy)_3^{2+}$ in zeolite-Y.[5] Since then, several publications have explored the chemistry of this and similar intrazeolitic complexes.[6] In hydrated zeolite, the observed spectroscopic properties of the encapsulated $Ru(bpy)_3^{2+}$ suggest that its structure is identical to that of the free complex in aqueous solution.[6]

Reaction of $Ru(bpy)_3^{3+}$−Y with Water. After production of the $Ru(bpy)_3^{3+}$ by Cl_2 oxidation, the zeolite samples were evacuated to remove excess Cl_2 and then immediately exposed to aqueous solutions of different pH. These included 10^{-4} M HCl (pH 4), deionized water (pH 7), and 10^{-2} M NaOH (pH 12). Since the zeolite matrix is hydrophilic, the hydration of the evacuated zeolite samples leads to immediate uptake of water within the zeolite pore system. However, in the case of the 10^{-4} M HCl solution, there is also the necessity of ion exchange of the protons. On the basis of previous experience with the ion exchange of monovalent ions and other reports,[9] we estimate a time of 30 min for equilibration. In the case of exposure to 0.01 M NaOH, we are limited to diffusion of $Na^+\cdots OH^-$ ion pairs for transport of the negatively charged hydroxide into the negatively charged aluminosilicate framework. As a result, only a fraction of the OH^- ions in solution are transported into the zeolite. Since this fraction is undetermined, we have no way of establishing the actual concentration of hydroxide ions in the zeolite. Thus, even though we identify the samples exposed to these solutions as "pH 4" and "pH 12" in the rest of this study, these labels only imply that the intrazeolite is in one case more acidic than those exposed to deionized water and in the other case more basic. The progress of the reaction was monitored by diffuse reflectance, resonance Raman, and EPR spectroscopies of the zeolite-entrapped ruthenium.

(a) Diffuse Reflectance Spectra. The diffuse reflectance signal comes from the surface layers of the zeolite, with photon penetration depths of submicrons. Figure 1 shows the evolution with time of the electronic spectra of $Ru(bpy)_3^{3+}$−Y after exposure to aqueous solutions of pH 4, 7, and 12. In each case, an insert shows the spectral activity in the 600−850-nm region. Data were taken more frequently than indicated, but excluded from the figure for clarity. Trace e in each case shows the spectra of $Ru(bpy)_3^{2+}$ in the zeolite used as starting material for generation of Ru(III). It is characterized by the MLCT band at 450 nm which resembles that observed in solution.[10] When the sample is dehydrated and exposed to Cl_2 gas as originally reported by Quayle and Lunsford,[1f] oxidation of the orange $Ru(bpy)_3^{2+}$ to the green $Ru(bpy)_3^{3+}$ is observed visually. The diffuse reflectance spectrum of $Ru(bpy)_3^{3+}$−Y is shown in trace a in each case. It is characterized by bands at 420 and 660 nm and is identical to the spectrum observed in solution.[11] These bands are assigned to charge transfer transitions from the bipyridyl π ligands to the electron deficient metal (t_{2g}).[11] The absence of the 450-nm band of $Ru(bpy)_3^{2+}$ upon oxidation confirms that the oxidation is complete within 1 h. This is in contrast with the high-loading samples examined by Quayle and

(5) DeWilde, W.; Peeters, G.; Lunsford, J. H. *J. Phys. Chem.* **1980**, *84*, 2306.

(6) (a) Dutta, P. K.; Turbeville, W. *J. Phys. Chem.* **1992**, *96*, 9410. (b) Turbeville, W.; Robins, D. S.; Dutta, P. K. *J. Phys. Chem.* **1992**, *96*, 5024. (c) Incavo, J. A.; Dutta, P. K. *J. Phys. Chem.* **1990**, *94*, 3075. (d) Dutta, P. K.; Incavo, J. A. *J. Phys. Chem.* **1987**, *91*, 4443. (e) Maruszewski, K.; Strommen, D. P.; Kincaid, J. R. *J. Am. Chem. Soc.* **1993**, *115*, 8345. (f) Maruszewski, K.; Strommen, D. P.; Handrich, K.; Kincaid, J. R. *Inorg. Chem.* **1991**, *30*, 4579.

(7) Kortum, G. *Reflectance Spectroscopy, Principles, Methods and Applications*; Springer-Verlag: Berlin, 1969.

(8) Breck, D. W. *Zeolite Molecular Sieves*; Wiley: New York, 1974.

(9) (a) Brigham, E. S.; Snowden, P. T.; Kim, Y. I.; Mallouk, T. E. *J. Phys. Chem.* **1993**, *97*, 8650. (b) Dutta, P. K.; Borja, M. *J. Chem. Soc., Chem. Commun.* **1993**, 1568. (c) Dutta, P. K.; Del Barco, B. *J. Chem. Soc., Chem. Commun.* **1985**, 1297.

(10) (a) Demas, J. N.; Crosby, G. A. *J. Mol. Spectrosc.* **1968**, *26*, 72. (b) Harrigan, R. W.; Crosby, G. A. *J. Chem. Phys.* **1973**, *59*, 3468.

(11) Braddock, J. N.; Meyer, T. J. *J. Am. Chem. Soc.* **1973**, *95*, 3158.

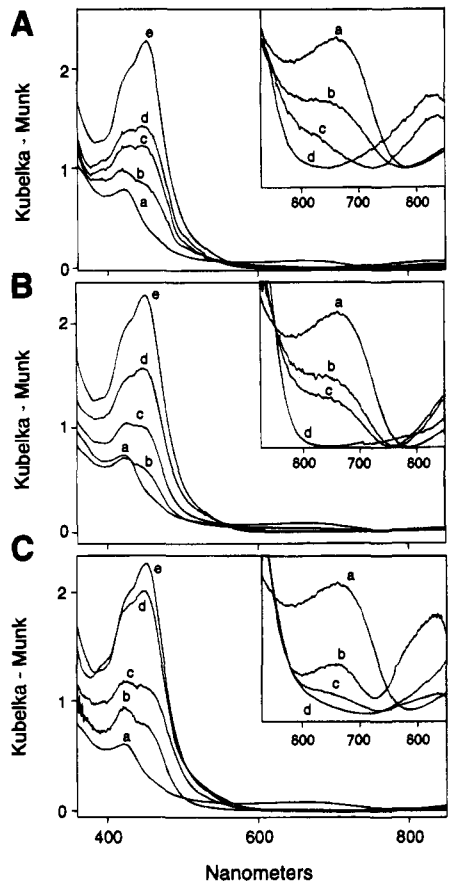

Figure 1. Diffuse reflectance spectra of $Ru(bpy)_3^{3+}$−zeolite Y-(A): exposed to pH 4 aqueous solution for various times [(a) 0 h, (b) 2 h, (c) 9 h, (d) 62 h] and (e) the initial $Ru(bpy)_3^{2+}$−zeolite-Y from which the $Ru(bpy)_3^{3+}$−zeolite-Y was formed; (B) exposed to deionized water (pH 7) for various times [(a) 0 h, (b) 1 h, (c) 10 h, (d) 42 h] and (e) the initial $Ru(bpy)_3^{2+}$−zeolite-Y; and (C) exposed to pH 12 aqueous solution for various times [(a) 0 h, (b) 1 h, (c) 4 h, (d) 15 h] and (e) the initial $Ru(bpy)_3^{2+}$−zeolite-Y.

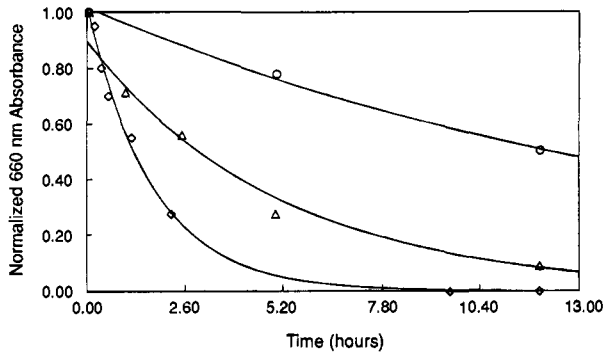

Figure 2. Decay of the LMCT band (660 nm) intensity of $Ru(bpy)_3^{3+}$−zeolite-Y at various pH's: (○) pH 4, (△) pH 7, (◇) pH 12.

Lunsford,[1f] in which prolonged Cl_2 exposure (>4 h) only resulted in ~85% oxidation.

Comparison of the intensity of the 450-nm MLCT band of the starting material (trace e in each case) with that after reaction with the aqueous solutions reveals that only a fraction of the $Ru(bpy)_3^{2+}$ is being recovered at pH 4 and 7, even after tens of hours. At pH 12, the recovery of the $Ru(bpy)_3^{2+}$ appears complete in 24 h. The decay of $Ru(bpy)_3^{3+}$ was monitored by following the decrease in intensity of the LMCT 660-nm band. Figure 2 illustrates the 660-nm decay over the first 13 h of reaction for each pH. It is clear that the Ru(III) reacts faster at higher pH, and over the 13 h period, the disappearance of $Ru(bpy)_3^{3+}$ is a first-order process in all three cases. The corresponding rate constants are as follows: pH 4, $k = 1.6 \times 10^{-5}$ s^{-1}; pH 7, $k = 5.7 \times 10^{-5}$ s^{-1}; pH 12, $k = 1.6 \times 10^{-4}$ s^{-1}.

There is also significant spectral activity in the 800−850-nm region. At pH 4 (Figure 1A), a broad band centered at 830 nm appears. Initially, the intensity of this band grows and after 20 hours is fairly constant with time, indicating that the product to which it corresponds is stable at this pH. At pH 7 (Figure 1B), there is a slow and sustained growth in intensity in the 850-nm region, but no resolved bands appear, indicating that one or more long-wavelength (λ > 850 nm) products are accumulating. Our instrument limits the long-wavelength measurement to 850 nm. At pH 12, the 830-nm band, which was stable at pH 4, grows for an hour (Figure 1C) and then rapidly decays, indicating that consumption of this intermediate is base dependent.

There have been several studies of hydroxylated bipyridine complexes of $Ru^{2+/3+}$ and $Fe^{2+/3+}$, all of which exhibit weak ($\epsilon \approx 1000$ M^{-1} cm^{-1}) absorption bands in the region between 750 and 850 nm.[1abg,12a] Similar hydroxylated complexes are also known to result from water attack on $Ru(bpy)_3^{3+}$,[1] and in one case the covalent hydrate of $Ru(bpy)_3^{3+}$ was isolated and characterized.[1g] Thus, it is reasonable to assign the λ > 800 nm absorptions observed here to at least two different hydroxylated $Ru(bpy)_3^{2+/3+}$ species. One of these is resolved at 830 nm and is stable at lower pH. The other(s) absorbs beyond 850 nm. Contributions of any of these species in the 400−500-nm region is difficult to discern because of the residual absorption from the Ru(III) species as well as contributions from the regenerated Ru(II) complex. More detailed assignments will be provided upon correlation of these observations with the EPR data.

(b) Resonance Raman Spectroscopy. Resonance Raman spectra of the $Ru(bpy)_3^{3+}$−Y sample after exposure to water at pH 7 were obtained over the range of 600−1700 cm^{-1} with 406.7-nm excitation. Each spectrum took about 40 min to obtain. The recording of spectra was begun after exposure to water for the period of time by which the sample is identified. These spectra are shown in Figure 3. For the sample hydrated for 140 min (Figure 3c), the spectrum that emerges is similar to that of $Ru(bpy)_3^{2+}$ (Figure 3d) with peaks at 1032, 1182, 1274, 1324, 1496, 1566, and 1612 cm^{-1}. Clearly at this point enough $Ru(bpy)_3^{2+}$ has been regenerated to dominate the resonance Raman spectrum. At the earliest times (Figure 3a), the spectrum is quite different, lacking the characteristic peaks and intensity ratio of $Ru(bpy)_3^{2+}$ in the ring breathing region (~1400−1700 cm^{-1}). Woodruff and co-workers have reported that the Raman spectrum of $Ru(bpy)_3^{3+}$ is similar to that of the divalent complex.[13] Clearly we are observing the spectra of some intermediate form.

Raman studies by Basu et al. have shown that substituents which significantly disturb the aromatic π system of bipyridine, such as $-NO_2$, alter the electronic and Raman spectra considerably.[14] These authors note that upon introduction of $-NO_2$ onto the ring, a red shift of the MLCT band to 486 nm is observed. Williams and co-workers reported that a "purple", covalently

(12) (a) Dimitrijevic, N. M.; Micic, O. I. *J. Chem. Soc., Dalton Trans.* **1982**, 1953. (b) Neta, P.; Silverman, J.; Markovic, V.; Rabani, J. *J. Phys. Chem.* **1986**, *90*, 703. (c) Heath, G. A.; Yellolees, L. J. *J. Chem. Soc., Chem. Commun.* **1981**, 287. (d) Tait, C. D.; Vess, T. M.; DeArmond, M. K.; Hanck, K. W.; Wertz, D. W. *J. Chem. Soc., Dalton Trans.* **1987**, 2467. (e) Heath, G. A.; Yellowlees, L. J. *Chem. Phys. Lett.* **1982**, *92*, 646.

(13) Bradley, P. G.; Kress, N.; Hornberger, B. A.; Dallinger, R. F.; Woodruff, W. H. *J. Am. Chem. Soc.* **1981**, *103*, 7441.

(14) Basu, A.; Gafney, H. D.; Strekas, T. C. *Inorg. Chem.* **1982**, *21*, 2231.

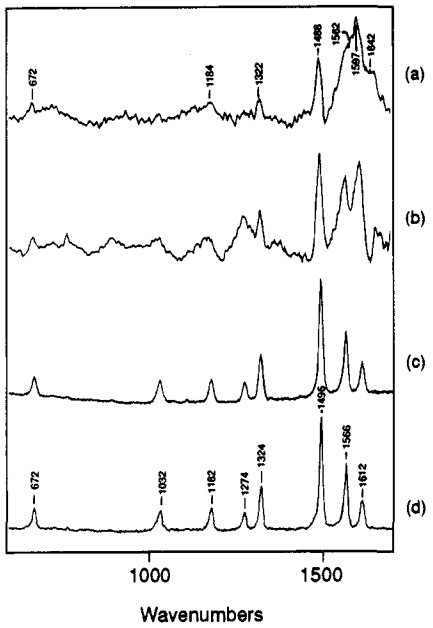

Figure 3. Resonance Raman spectra of $Ru(bpy)_3^{3+}$−zeolite after exposure to water (pH 7) for (a) 10 min, (b) 80 min, and (c) 140 min and (d) initial $Ru(bpy)_3^{2+}$−zeolite-Y sample.

hydrated, $Ru(bpy)_2(bpy{\cdot}H_2O)^{3+}$ absorbs at 472 nm.[1g] In the electronic spectra (Figure 1), we cannot explicitly distinguish a band in this region, though there is intensity enhancement in the 480-nm region. Also, the infrared spectrum of the "purple" complex shows alterations in the frequencies and intensities of the C=N and C=C stretching frequencies in the 1400−1500-cm^{-1} region.[1g] In the Raman spectrum, we observe changes in the 1400−1600-cm^{-1} region, also assigned to C=N and C=C stretching vibrations.[15] Bands are at 1488, 1562, 1597, and 1642 cm^{-1} and the intensity pattern resembles that of the nitro complex. This example of the nitro derivative illustrates that distinct vibrational alterations occur in the $Ru(bpy)_3^{2+}$ system if the π system of the bipyridine ligand is altered. We propose that the Raman spectral changes at the earliest times after exposure to water arise from formation of the covalent hydrate. This substitution would perturb the aromaticity of the bipyridine ring and is expected to change the vibrational spectrum.

(c) EPR Studies. EPR spectra of the $Ru(bpy)_3^{3+}$−Y samples exposed to water at the various pH's were examined as a function of time. The data obtained at pH 4 and 7 are shown in Figure 4 and those at pH 12 are shown in Figure 5. In Figure 4II inserts magnify the $g \approx 2$ region. We must stress that the time dependence observed in the EPR spectra cannot be compared directly with that observed for the diffuse reflectance spectra. This arises from the partial dehydration step required to obtain the EPR spectra. The resultant decrease in the zeolite water content accentuates the intrazeolitic pH, increasing the activity of trapped protons or hydroxides. In effect, basic samples are made more basic, acidic samples are made more acidic, and the overall reaction rate is altered. Since this effect could not be quantified, the EPR data are used only to show the evolution of radical intermediates. However, the EPR spectra observed at the various pH's can be compared with each other, since the experimental conditions were similar. It should be noted that the relative reaction rates observed are consistent between both EPR and diffuse reflectance data, both showing that the rate of reduction of $Ru(bpy)_3^{3+}$ increases with pH.

(15) Mallick, P. K.; Danzer, G. D.; Strommen, D. P.; Kincaid, J. R. *J. Phys. Chem.* **1988**, *92*, 5628.

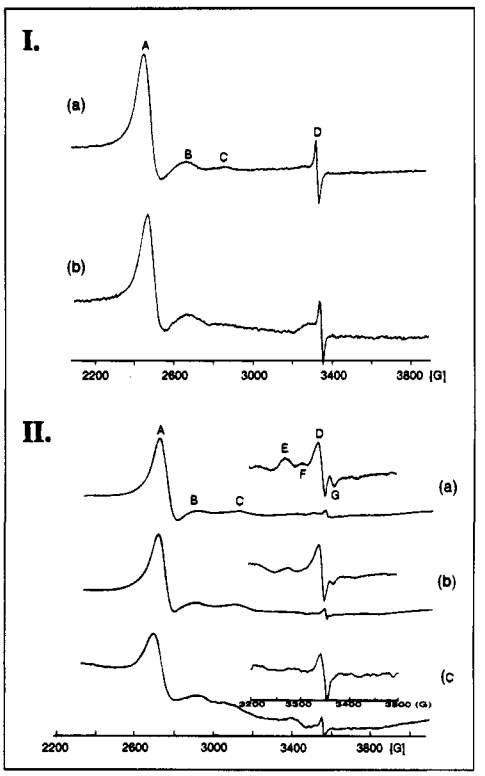

Figure 4. EPR spectra of $Ru(bpy)_3^{3+}$−zeolite-Y after exposure to aqueous solution at (I) pH 4 for (a) 25 min and (b) 6 h and (II) at pH 7 for (a) 20 min, (b) 2 h, (c) 9 h.

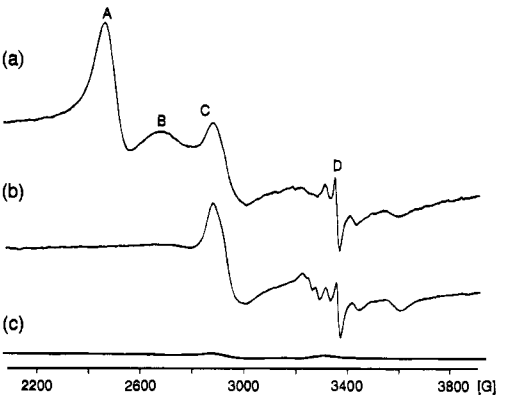

Figure 5. EPR spectra of $Ru(bpy)_3^{3+}$−zeolite-Y after exposure to aqueous solution at pH 12 for (a) 20 min, (b) 1 h, and (c) 6 h.

The relevant EPR activity in Figures 4 and 5 is confined to two distinct regions of the spectrum. Metal-centered radicals resonate in the range of 2400−3000 G which corresponds to g values of ~2.7−2.3.[16] Ligand-centered radicals are observed in the free electron region, between 3200 and 3500 G ($g \sim 2$).[16]

(16) (a) Tanaka, N.; Ogata, T.; Niizuma, S. *Bull. Chem. Soc. Jpn.* **1973**, *46*, 3299. (b) Morris, D. E.; Hanck, K. W.; DeArmond, M. K. *J. Am. Chem. Soc.* **1983**, *105*, 3032. (c) DeArmond, M. K.; Hanck, K. W.; Wertz, D. W. *Coord. Chem. Rev.* **1985**, *64*, 65. (d) Motten, A. G.; Hanck, K.; DeArmond, M. K. *Chem. Phys. Lett.* **1981**, *79*, 541. (e) DeSimone, R. E. *J. Am. Chem. Soc.* **1973**, *95*, 6238. (f) DeSimone, R. E.; Drago, R. S. *J. Am. Chem. Soc.* **1970**, *92*, 2343. (g) Kaim, W.; Ernst, D.; Kohlmann, S.; Welkerling, P. *Chem. Phys. Lett.* **1985**, *118*, 431. (h) Morris, D. E.; Hanck, K. W.; DeArmond, M. K. *Inorg. Chem.* **1985**, *24*, 977. (i) Goldwasser, M.; Dutel, J. F.; Naccache, C. *Zeolites* **1989**, *9*, 54. (j) Kaim, W.; Ernst, S.; Kasack, V. *J. Am. Chem. Soc.* **1990**, *112*, 173. (k) Kaim, W.; Ernst, S. *J. Phys. Chem.* **1986**, *90*, 5010. (l) Rose, D.; Wilkinson, G. *J. Chem. Soc. A* **1970**, 1791. (m) Gregson, A. K.; Mitra, S. *Chem. Phys. Lett.* **1969**, *3*, 392. (n) Bunker, B. C.; Drago, R. S.; Hendrickson, D. N.; Richman, R. M.; Kessell, S. L. *J. Am. Chem. Soc.* **1978**, *100*, 3805.

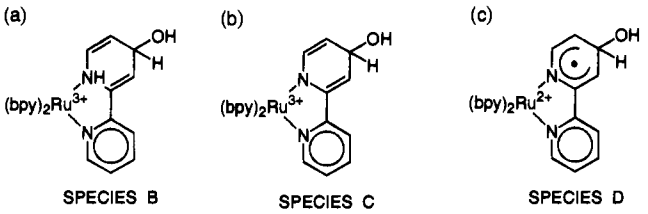

Figure 6. Structure of intermediates B, C, and D observed in the spectroscopic studies.

The band at $g = 2.63$ (A), observed initially as the strongest signal at all pH's, is assigned to $Ru(bpy)_3^{3+}$. This is consistent with the work of DeSimone and Drago,[16f] as well as Quayle and Lunsford's highly loaded $Ru(bpy)_3^{3+}$ in zeolite-Y.[1f] Confirmation of this assignment is obtained by scanning the region beyond 9000 G, where the $g_{\|}$ component is readily observable at $g = 1.14$. The magnitude of the **g** tensor for radical A is indicative of a spin largely localized on metal-centered orbitals.[16] Signal A is always present in the EPR spectra of the "pH 4" and "pH 7" samples, but it is not observed beyond the first hour in the "pH 12" sample, indicating that reaction of $Ru(bpy)_3^{3+}$ is promoted by base, in agreement with the diffuse reflectance data.

There are two other signals in the metal centered region at $g = 2.46$ (B) and 2.28 (C). These were also observed by Quayle and Lunsford[1f] upon exposure of the highly loaded $Ru(bpy)_3^{3+}$ zeolite-Y to water and assigned simply to Ru(III) species. That assignment was based on the work by Williams and co-workers in which prolonged chlorine oxidation of aqueous $Ru(bpy)_3^{2+}$ produced a covalent ligand hydrate. This was isolated and assigned as $Ru^{3+}(bpy)_2(bpy{-}OH_2)$.[1g] That compound was EPR active with a broad signal at the reduced g value around 2.3,[1g] indicative of increased covalency (with respect to A) in the Ru−N bond and thought to be brought about by the increased electron density on the hydrated ligand.[16] In the zeolite, we assign the signal at $g = 2.46$ (B) to the covalent hydrate of $Ru(bpy)_3^{3+}$, illustrated in Figure 6a. The Raman spectrum obtained upon brief exposure to water and the long-wavelength electronic bands (>850 nm) also support the formation of this hydrate. This intermediate is the product of a water attack at either the 2,2′ or 4,4′ carbon of a bipyridyl ligand, a process that has been proposed as the initial reaction for aqueous reduction of $Ru(bpy)_3^{3+}$ in a number of studies.[1a,b,e-g]

$$\underset{\text{A}}{Ru(bpy)_3^{3+}} + H_2O \rightarrow \underset{\text{B}}{Ru^{3+}(bpy)_2(bpy{-}OH_2)} \quad (1)$$

The EPR signal near $g = 2.3$ becomes the most prominent signal in the pH 12 sample after 1 h, while it remains weak relative to signal A in the pH 4 sample. This indicates that the formation of this species is promoted by base. The covalent hydrate assigned to signal B can readily deprotonate in basic medium to form C according to

$$\underset{\text{B}}{Ru^{3+}(bpy)_2(bpy{-}OH_2)} + OH^- \rightarrow \underset{\text{C}}{Ru^{3+}(bpy)_2(bpy{-}OH^-)} + H_2O \quad (2)$$

Since there is increased electron density at the coordinating nitrogen upon deprotonation, the EPR signal of C is shifted toward lower g values. Intermediate C is illustrated in Figure 6b. Thus, we propose that although initially the covalent hydrate (B) is formed at all pH's, in the presence of base, deprotonation drives reaction 2 to the right. Eventually, at pH = 12, all of the signal due to the starting $Ru(bpy)_3^{3+}$ (A) disappears.

Several signals are also observed in the $g = 2.0$ region. We begin the assignment with the signal at $g = 2$ marked as D on the EPR spectra at pH = 4 (Figure 4I). In previous studies, the pseudobase C was assumed to undergo intramolecular electron transfer, generating Ru(II) and a ligand-based radical.[1a,b,e-g] We assign signal D to this ligand-based radical.

$$\underset{\text{C}}{Ru^{3+}(bpy)_2(bpy{-}OH^-)} \rightarrow \underset{\text{D}}{Ru^{2+}(bpy)_2(bpy{-}OH^{\bullet})} \quad (3)$$

Intermediate D is illustrated in Figure 6c. The assignment of D to this carbon radical is based on the magnitude of the **g** tensor, as well as the observed symmetry and line width of the signal, all of which are consistent with previously observed ligand-based radicals of ruthenium polypyridyls.[16] In D, a hydroxylated bipyridine radical is ligated to Ru(II). Such a species has been made by pulse radiolysis, the reaction of bipyridyl ligands of $Ru(bpy)_3^{2+}$ with $OH^{\bullet}$ being quite facile.[1b] In solution this complex has been shown to decay by a second-order process in the time range of 0.1−100 ms (6×10^6 M^{-1} s^{-1}).[12b] The products of these reactions were not identified. However, in the zeolite multimolecular processes are eliminated by encapsulation, and the radical is observed to be quite stable.

Further examination of the $g = 2$ region at the early stages of the pH 7 and pH 12 samples clearly indicates that there are other species present. In Figure 4II, the signal at $g = 2.047$ (E) is indicative of the g_1 component of superoxide ($O_2^{\bullet-}$) in zeolites and silica matrices,[17] and is thus assigned. A g_2 component, expected at $g \sim 2.00$, overlaps with signal D and is unresolved. Concentrating on Figure 4II, an interesting feature is the pair of signals F and G, which disappear with time. These are characteristic of hydroxyl radical ($OH^{\bullet}$, or O^-) absorbed to silica, trapped in aqueous glass or polycrystalline ice.[18] The $g \sim 2.00$ component expected from the hydroxyl radical again overlaps with signal D, thus the characteristic 40 G doublet splitting is difficult to discern. Corresponding signals are also observed in the pH 12 sample. Because hydroxyl radical is so reactive, it was surprising to find signals that fit its pattern. We attempted to confirm the presence of $OH^{\cdot}$ by trapping it with the DMPO spin trap. The reaction of $Ru(bpy)_3^{3+}$−Y with water was carried out in the presence of DMPO, which should bind free $OH^{\bullet}$.[19] EPR spectra were recorded at various times and the spectrum in the $g = 2$ region after 4 h of reaction is shown in Figure 7a. Also shown in Figure 7b is the spectrum derived by subtracting from the 4 h DMPO spectrum a spectrum obtained in the absence of DMPO. The presence of the bipyridyl-based signal (D) and the superoxide complicates the analysis. However, in the presence of DMPO, there is clearly the appearance of a signal which shows four peaks with a 14.5 G splitting pattern characteristic of the DMPO−OH adduct.[19] This is a strong indication that oxygen radical species are being formed as intermediates. Hydroxyl radical would be the product of the following reaction:

$$\underset{\text{D}}{Ru^{2+}(bpy)(bpy{-}OH^{\bullet})} \rightarrow Ru(bpy)_3^{2+} + \underset{\text{F, G}}{OH^{\bullet}} \quad (4)$$

(17) (a) Chamulitrat, W.; Kevan, L. *J. Phys. Chem.* **1985**, *89*, 4989. (b) Howe, R. F.; Timmer, W. C. *J. Chem. Phys.* **1986**, *85*, 6129. (c) Min-Ming, H.; Johns, J. R.; Howe, R. F. *J. Phys. Chem.* **1988**, *92*, 1291. (d) Kasai, P. H. *J. Chem. Phys.* **1965**, *43*, 3322.

(18) (a) Bednarek, J.; Schlick, S. *J. Phys. Chem.* **1991**, *95*, 9940. (b) Riederer, H.; Hüttermann, J. *J. Magn. Reson.* **1983**, 54. (c) Brivati, J. A.; Symons, C. R.; Tinling, H. W.; Wardale, H. W.; Williams, D. O. *J. Chem. Soc.* **1965**, 402.

(19) (a) Finkelstein, E.; Rosen, G. M.; Rauckman, E. J. *Arch. Biochem. Biophys.* **1980**, *200*, 1. (b) Janzen, E. G.; Nutter, D. E.; Davis, E. R.; Blackburn, B. J. *Can. J. Chem.* **1978**, *56*, 2237.

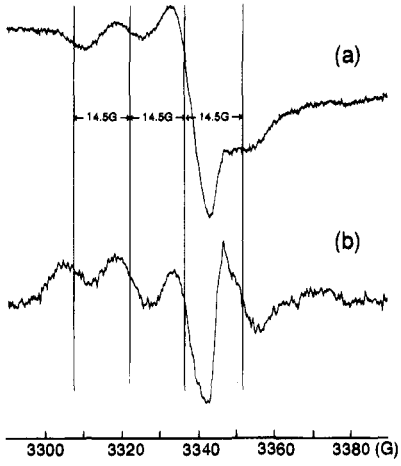

Figure 7. (a) EPR spectrum of $Ru(bpy)_3^{3+}$−zeolite-Y exposed to and aqueous solution of DMPO for 4 h. (b) Spectrum obtained by subtraction of Figure 7a from a sample that was run in the absence of DMPO.

Once generated, the free hydroxyl can either attack the complex from which it was formed (i.e. the reverse reaction) or diffuse through the zeolite and attack the first organic species it encounters. As pointed out earlier, a great deal of effort was expended in order to ensure that the samples were free of excess organic ligands. Therefore, the free OH• is forced to attack a ruthenium complex. Previous studies have shown the propensity of the hydroxyl radical to bind to bipyridyl ligand.[12] We have already suggested the presence of three different ruthenium radicals (A, B, C), their relative concentrations being a function of reaction time and pH. At low pH, and at the earliest stages at higher pH, unreacted $Ru(bpy)_3^{3+}$ (A) will predominate. Hydroxyl radical attack on unreacted $Ru(bpy)_3^{3+}$ should result in a biradical molecule (H) with spins on the ligand and the metal ion.

$$\underset{A}{Ru(bpy)_3^{3+}} + OH^{\bullet} \rightarrow \underset{H}{Ru^{3+}(bpy)_2(bpy{-}OH^{\bullet})} \qquad (5)$$

Strong coupling is expected for such complexes, resulting in a singlet state.[20d] This would make it difficult to detect by EPR spectroscopy. Reaction 5 has been studied by pulse radiolysis[1a,b] and is known to be quite fast. The product has a visible absorption at $\lambda > 800$ nm and a pK_a of ~13.5.[1a] Bands in this region are observed in this study. Since other hydroxylated bipyridine ligands also absorb in this region, we cannot assign definite bands to species H.

Dioxygen Evolution. The evolution of O_2 from the reaction of $Ru(bpy)_3^{3+}$ with water was measured at the various pH's by gas chromatographic analysis of the headspace above the hydrated samples. Even under double enclosure conditions, minute amounts of air leaked into the system over the 24 h reaction period. Thus, the oxygen content was estimated by difference. Assuming that all the N_2 observed is from air, we can calculate the amount of O_2 from leaked air and subtract this amount from the observed O_2 signal. Figure 8A shows the GC trace of a typical pH 12 sample overlaid with an air blank. In this case the blank was prepared by sealing an empty reaction vessel within the glovebag at the same time the pH 12 sample was prepared.

Confirmation that the O_2 observed via GC arises from the oxidation of water was obtained by mass spectroscopy. The

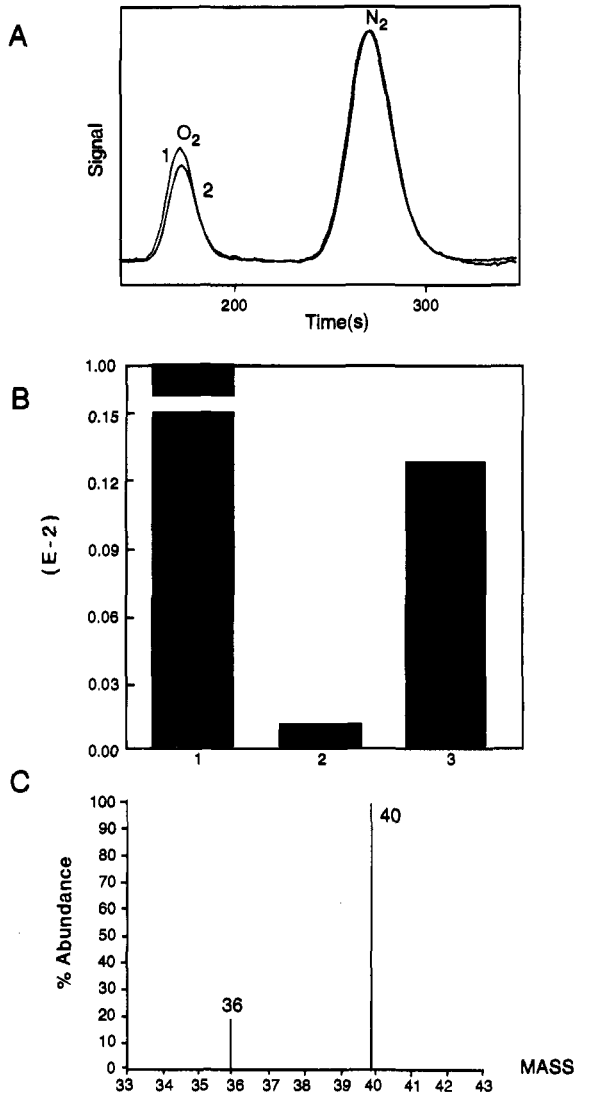

Figure 8. (A) Gas chromatographic trace of the headspace of (1) $Ru(bpy)_3^{3+}$−zeolite-Y at pH 12 after 24 h and (2) a similar experiment with a blank sample. (B) Comparison of the mass spectral signal at (1) $m/z = 32$ (normalized) with $m/z = 36$ for the gas in the headspace over a (2) zeolite sample and $H_2{}^{18}O$ water and (3) $Ru(bpy)_3^{3+}$−zeolite and $H_2{}^{18}O$ water sample. (C) Mass spectra of 1 μL of $H_2{}^{18}O$ taken from a $Ru(bpy)_3^{3+}$−zeolite and $H_2{}^{18}O$ water sample.

sample was hydrated with 99% $H_2{}^{18}O$ and allowed to react in the septum-equipped reactor. After 24 h the mass spectrum of the vapor phase was analyzed, and in all cases the ratio of the mass 36 peak (due to $^{18}O_2$) to the mass 32 peak (due to $^{16}O_2$) was at least an order of magnitude higher than that observed for a zeolite sample without the ruthenium complex. These data are shown as a histogram in Figure 8B. In addition, the $H_2{}^{18}O$ was directly injected into a high-resolution mass spectrometer. A signal at 35.9994 due to $^{18}O_2$ was observed in the sample containing $Ru(bpy)_3^{3+}$, but not in the $H_2{}^{18}O$ blank. A typical mass spectrum for the water sample containing $Ru(bpy)_3^{3+}$−zeolite-Y sample is shown in Figure 8C, with the mass at 36 due to $^{18}O_2$. The mass at ~40 also observed in the blank is arising from argon, a component of air that is leaking into the sample (peaks due to N_2 and $^{16}O_2$ were also observed). Clearly, in the presence of zeolite-entrapped $Ru(bpy)_3^{3+}$, dioxygen is being formed from water.

The oxidation of water to dioxygen is a 4-electron process, requiring 4 mol of $Ru(bpy)_3^{3+}$ to generate 1 mol of O_2. Taking this into account, we calculated the fraction of the original $Ru(bpy)_3^{3+}$ that results in O_2 evolution from the GC data. These

(20) (a) Lay, P. A. *Inorg. Chem.* **1984**, *23*, 4775. (b) Serpone, N.; Ponterini, G.; Jamieson, M. A. *Coord. Chem. Rev.* **1983**, *50*, 209. (c) Gillard, R. D. *Coord. Chem. Rev.* **1975**, *16*, 67. (d) Kaim, W. *Coord. Chem. Rev.* **1987**, *76*, 187.

Scheme 1

$$\underset{A}{Ru(bpy)_3^{3+}} + H_2O \rightarrow \underset{B}{[Ru^{3+}(bpy)_2(bpy\text{–}H_2O)]^{3+}} \quad (1)$$

$$\underset{B}{[Ru(bpy)_2(bpy\text{–}H_2O)]^{3+}} \xrightarrow[OH^-]{} \underset{C}{[Ru^{3+}(bpy)_2(bpy\text{–}OH^-)]^{2+}} + H_2O \quad (2)$$

$$\underset{C}{[Ru^{3+}(bpy)_2(bpy\text{–}OH^-)]^{2+}} \rightarrow \underset{D}{[Ru^{2+}(bpy)_2(bpy\text{–}OH^{\bullet})]^{2+}} \quad (3)$$

$$\underset{D}{[Ru(bpy)_2(bpy\text{–}OH^{\bullet})]^{2+}} \rightarrow Ru(bpy)_3^{2+} + \underset{F,G}{OH^{\bullet}} \quad (4)$$

$$\underset{A}{Ru(bpy)_3^{3+}} + \underset{F,G}{OH^{\bullet}} \rightarrow \underset{H}{[Ru^{3+}(bpy)_2(bpy\text{–}OH^{\bullet})]^{3+}} \quad (5)$$

$$\underset{H}{[Ru^{3+}(bpy)_2(bpy\text{–}OH^{\bullet})]^{3+}} + OH^- \rightarrow Ru(bpy)_3^{2+} + H_2O_2 \quad (6)$$

$$\underset{C}{[Ru^{3+}(bpy)^2(bpyOH^-)]^{2+}} + \underset{F,G}{OH^{\bullet}} \rightarrow Ru(bpy)_3^{2+} + H_2O_2 \quad (6')$$

$$\underset{A}{Ru(bpy)_3^{3+}} + H_2O_2 \rightarrow Ru(bpy)_3^{2+} + \underset{E}{O_2^-} + 2H^+ \quad (7)$$

$$\underset{A}{Ru(bpy)_3^{3+}} + O_2^- \rightarrow Ru(bpy)_3^{2+} + O_2 \quad (8)$$

$$\underset{C}{[Ru^{3+}(bpy)_2(bpy\text{–}OH^-)]^{2+}} + H_2O_2 \rightarrow Ru(bpy)_3^{2+} + O_2^- + H_3O^+ \quad (9)$$

$$\underset{C}{[Ru^{3+}(bpy)_2(bpy\text{–}OH^-)]^{2+}} + O_2^- \rightarrow Ru(bpy)_3^{2+} + O_2 + OH^- \quad (10)$$

results were the following: the "pH 4" sample showed ~0% conversion of $Ru(bpy)_3^{3+}$ to O_2; "pH 7" showed 30–50% conversion; and pH 12 showed 70–90% conversion. As shown earlier, the diffuse reflectance and EPR studies show that complete recovery of $Ru(bpy)_3^{2+}$ is only observed at high pH. Thus, these results are consistent with a mechanism in which a major portion of the $Ru(bpy)_3^{3+}$ which is reduced at high pH's results in formation of O_2.

Discussion

These data support the conclusion that water can be oxidized to dioxygen by intrazeolitic $Ru(bpy)_3^{3+}$, and that the completion of this reaction is strongly base dependent. With this result as our basis, there are four issues which are addressed. First, we propose a mechanism that is consistent with the pH effects and the proposed intermediates. Second, we contrast the present study with that of Quayle and Lunsford[1f] in highly loaded zeolites, justifying the vastly different chemistry observed. Third, we rationalize the differences between our intrazeolitic observations and the solution-based chemistry reported previously.[1] Finally, we investigate the possible role of intrazeolitic transition metal impurities in this chemistry.

Mechanism. The spectroscopic and chromatographic data presented earlier show the presence of a variety of reactants, products, and intermediates which were assigned and identified as A–G. Scheme 1 illustrates a mechanism which is consistent with these observations.

Reaction 1 was originally proposed by Creutz and Sutin[1a] and has been invoked as the initiating step in subsequent studies.[1b,d-g] "Quarternization" of the nitrogen by binding to the metal ion is proposed to activate the ligand to nucleophilic attack by water.[20] These water addition products are observed to have long-wavelength electronic absorption (λ > 850 nm) and EPR signals characteristic of metal-centered radicals.[1] The Raman spectra at the earliest times also show evidence of substitution on the bipyridyl ring. These properties are consistent with our assignment of intermediate B. Water addition can occur at the 2′ or 4′ positions, resulting in the intermediate illustrated in Figure 6a. We cannot distinguish spectrally between these two isomeric forms.

Reaction 2 involves deprotonation of the coordinated water and should therefore be pH dependent. The EPR spectra of the deprotonated form (C) is expected to be shifted downfield compared to the water adduct (B). The intensity of the EPR signal at $g = 2.28$ which is due to C increases gradually in the pH 12 sample, whereas the starting $Ru(bpy)_3^{3+}$ (A) signal completely disappears (Figure 5). For the pH 4 sample, reaction 2 does not occur to a great degree and the aquo complex (B) is primarily present, along with unreacted $Ru(bpy)_3^{3+}$. Comparison of the diffuse reflectance data with the EPR shows that the relative kinetic behavior of B is paralleled in the electronic spectrum by the 830-nm absorption. At pH 12 (Figure 1C), the 830-nm band maximizes early and is gone after 2 h, nearly identical to the behavior of B in the EPR. At pH 4 (Figure 2), the 830-nm band maximizes and remains relatively constant. Again, this is analogous to the EPR behavior of B in the pH 4 sample (Figure 7). Thus, the presence of base promotes the conversion of $Ru(bpy)_3^{3+}$ completely to the hydroxide adduct.

Reaction 3 is an intramolecular electron transfer step. This reaction has been previously proposed for the solution-based chemistry of $Ru(bpy)_3^{3+}$,[1b,e-g] and was described as facile. In these studies, a large rate constant was observed for radiolytic hydroxyl radical addition to $Ru(bpy)_3^{2+}$ and trivalent ruthenium was not observed as a product. Based on these observations, it was determined that intramolecular electron transfer from hydroxide to Ru(III) was a facile process.[1b,e,f] Examination of reaction 3 shows that it represents the initiation of the thermodynamically unfavorable oxidation of OH^- to $OH^{\bullet}$. The product of reaction 3 is a relatively stable, ligand-centered radical assigned as D. This assignment is consistent with previous work in which ligand-centered radicals were generated electrochemically.[16] These radicals are characterized by symmetric EPR signals centered at $g = 2.00$, with line widths of ~50 G. This species also has electronic absorptions in the region >850 nm, and contributes to the absorbance observed in that region.

In reaction 4, we propose the generation of free hydroxyl radical via homolytic cleavage of the C–O bond. This has been proposed for a number of similar, solution-based systems,[1a,e,g] but hydroxyl radical has never before been detected. This is not surprising, considering the reactive nature of this radical. Also, the chemistry of D in aqueous solutions is dominated by multimolecular degradation. It is here that the zeolite architecture plays a crucial role. By trapping D within the supercage, multimolecular processes are eliminated, and reaction 4 can occur. Once generated, if the hydroxyl radical manages to escape from the supercage containing the $Ru(bpy)_3^{2+}$, it will diffuse through the zeolite. Evidence for the formation of free $OH^{\bullet}$ is provided by the EPR data. Signals F and G are characteristic of free hydroxyl radical,[18] while more convincing proof was provided by trapping the radical with DMPO. This is a logical conclusion considering that O_2 is generated. The oxidation process must proceed, or at least be initiated by, single electron steps, in which the oxidation of hydroxide to hydroxyl is a necessary first step.

Once free, the fate of the hydroxyl radical depends on the unreacted ruthenium species, which as we have noted before is determined by pH. At low to neutral pH, and at the earlier times at high pH, the hydroxyl is statistically most likely to encounter unreacted $Ru(bpy)_3^{3+}$ as it is the dominant organic containing species. This is illustrated in reaction 5.

The disappearance of species H is controlled by the pH. Reaction 6, a two-electron step in which 1 mol of OH^- and 1

mol of H are converted to the reduced Ru(II) metal complex and peroxide, results in the decay of H. This reaction has been proposed previously for hydroxylated bipyridine complexes of both Fe(III) and Ru(III), but it was not observed experimentally.[1a,e,14a] In the case of the iron complex, it was believed that ligand degradation was occurring in lieu of water oxidation.

Since reaction 2 is strongly pH dependent, but reactions 3–5 are not, at high pH there is rapid conversion of A to C, but a relatively slow conversion of C to H. This results in loss of A, and a buildup of C, illustrated in the EPR data in Figure 5. After A has completely transformed into C, the free hydroxyl generated in reaction 4 cannot go on to form H, but will instead react with C as this species now predominates. This is illustrated in reaction 6′, in which OH• attack on C results in a two-electron process analogous with reaction 6. Here peroxide is generated directly from the hydroxyl, bypassing reactions 5 and 6.

The formation of H_2O_2 begins to distinguish the high pH mechanism from the acidic pH reaction. Once the peroxo species has been generated, it rapidly reduces any of the ruthenium(III)-containing products to give superoxide[21] (assigned in the EPR as E), which can then reduce Ru(III) to give O_2 by the sequence of reactions 7 through 10, depending both on the extent of reaction 2 and the pH. This chemistry is well-known and can include intermediates HO_2^- and $HO_2^{\bullet}$.[21] At the intermediate pH of 7, reactions 2 and 6 are occurring to a larger degree than pH 4, but less so than at pH 12.

Taken together, these observations explain the observed pH dependence of dioxygen production. The spectroscopic data indicate that the reaction only proceeds to completion at high pH, consistent with the proposed mechanism in which reactions 2 and 6 are base dependent. Likewise, the amount of oxygen generated is proportional to the extent of reaction. At lower pH, the reaction stops, trapping the oxidizing intermediates, and generating less O_2. In the pH 4 sample, dioxygen is not observed because reaction 6 does not occur.

Correlation with Previous Studies. We now address the differences observed here with that of Quayle and Lunsford's pioneering work using $Ru(bpy)_3^{3+}$–zeolite-Y.[1f] It was reported that the Ru^{3+} signal in the EPR disappeared rapidly (<1 min) and completely upon exposure to "pH 7" water. They also observed the evolution of CO_2 but no O_2. There are three major differences between their material and that used in this study, which if taken collectively explain the observed differences. First, the electronic spectra reported by Quayle and Lunsford indicate that their samples contain a considerable amount of incompletely formed $Ru(bpy)_n^{2+}$ ($n = 1, 2$) and ruthenium "red" (absorbance around 520 nm). Careful manipulation of the $Ru(NH_3)_6^{3+}$ in an inert atmosphere minimized the formation of ruthenium red in this study. Also, extensive sodium ion exchange liberates the incompletely formed ruthenium complexes from the present sample. Second, considerable amounts of free bipyridine ligand are retained in the zeolite following the synthesis.[6a,b] Soxhlet extraction with methanol requires 4–5 weeks to remove the excess bipyridine. This complication was not recognized at the time of Quayle and Lunsford's work. Thus in their preparation, the unreacted ligand was not removed. Finally, their loading of ruthenium was sufficiently high (1 complex per 2.3 supercages) that neighboring cages contained ruthenium(III), facilitating multimolecular interactions. In the present case, with a loading of 1 Ru per 15 supercages, these multimolecular interactions are minimized. While Quayle and Lunsford's system resembles $Ru(bpy)_3^{3+}$ in solution with excess bipyridine ligand, the system described in this study approximates aqueous $Ru(bpy)_3^{3+}$ at infinite dilution. The direct reaction of $Ru(bpy)_3^{3+}$ with water is forced because all other pathways are eliminated.

(21) Macartney, D. H. *Can. J. Chem.* **1986**, *64*, 1937.

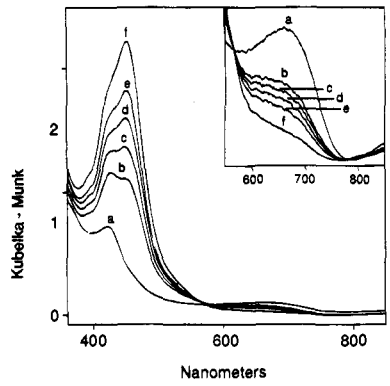

Figure 9. Diffuse reflectance spectra of $Ru(bpy)_3^{3+}$–Co^{2+}–zeolite-Y exposed to deionized water: (a) 0 h, (b) 30 min, (c) 90 min, (d) 2 h, (e) 3 h, and (f) 10 h.

The observation by Quayle and Lunsford regarding CO_2 as the major oxidation product is similar to what has been reported in aqueous solution.[1b] It is likely that reaction steps 1 through 3 shown in Scheme 1 are similar in all three cases, i.e. our low loading zeolite sample, Quayle and Lunsford's highly loaded and ligand-containing zeolite sample, and aqueous solutions of $Ru(bpy)_3^{3+}$ reported by Ghosh et al.[1b] Once generated in solution, or in highly loaded zeolite, C undergoes a fast bimolecular reaction with $Ru(bpy)_3^{3+}$. Such a step is the beginning of ligand dissociation to form species such as formic acid and formamide, as proposed by Ghosh et al.[1b] This step is eliminated in our system. In case reaction 4 does occur to some degree in Quayle and Lunsford's sample due to some fraction of isolated $Ru(bpy)_3^{3+}$, the OH• radical will immediately attack the excess bipyridine present in the cages and is not expected to form O_2. Thus, our success in making O_2 is made possible by eliminating the degradative steps through encapsulation.

Possible Role of Intrazeolitic Metal Impurities. It is well-established that transition metals can catalyze the oxidation of water by $Ru(bpy)_3^{3+}$.[1b,22] Since zeolites contain trace metal impurities such as iron and manganese, we investigated the possibility of metal-catalyzed reactions to explain our observations of O_2 formation. Among the metal ions reported in the literature as potential catalysts for this reaction, hydroxocobalt(II) complexes are the most effective.[22] Thus, we chose to examine the reaction of water (pH = 7) with $Ru(bpy)_3^{3+}$–zeolite-Y purposely loaded with hydrated Co(II). Cobalt ions were exchanged into $Ru(bpy)_3^{2+}$–Y, and the samples were oxidized with Cl_2, exposed to water, and examined by diffuse reflectance and EPR spectroscopy. The diffuse reflectance data after exposure to water (pH 7) are shown in Figure 9. The insert shows the decay in the 650-nm region. The reduction of $Ru(bpy)_3^{3+}$ is rapid and complete in the presence of intrazeolitic Co(II), but O_2 was not observed as a product. Also, long-wavelength intermediates were not observed in the electronic spectrum. The EPR spectra showed the complete disappearance of the Ru^{3+} signal within 10 h, and there was no indication of any Ru(III) intermediates. In Figure 10, the disappearance rate of the 660-nm band due to $Ru(bpy)_3^{3+}$ is compared with the appearance of the 450-nm band of $Ru(bpy)_3^{2+}$. The agreement

(22) (a) Brunschwig, B. S.; Chou, M. H.; Creutz, C.; Ghosh, P.; Sutin, N. *J. Am. Chem. Soc.* **1983**, *105*, 4832. (b) Wells, C. F. *Inorg. Chim. Acta* **1990**, *177*, 127. (c) Chandrasekharan, K.; Natarajan, P. *J. Chem. Soc., Dalton Trans.* **1981**, 478. (d) Anbar, M.; Pecht, I. *J. Am. Chem. Soc.* **1967**, *89*, 2553. (e) Shafirovich, V. Ya.; Khannonov, N. K.; Strelets, V. V. *Nouv. J. Chim.* **1980**, *4*, 81. (f) Shafirovich, V. Ya.; Strelets, V. V. *Nouv. J. Chim.* **1978**, *2*, 199.

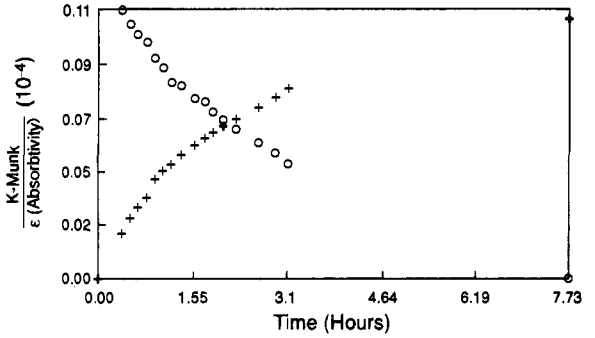

Figure 10. Dependence of the appearance of $Ru(bpy)_3^{2+}$ signal at 450 nm (+) contrasted with the decay of the $Ru(bpy)_3^{3+}$ signal at 660 nm (o).

of these rates coupled with the absence of intermediates suggests a direct outer-sphere electron transfer:

$$Co^{2+}-O-\text{zeolite} + Ru(bpy)_3^{3+} \rightarrow Co^{3+} + Ru(bpy)_3^{2+}$$

In solution, the reaction with hydrolyzed Co(II) was also proposed to be the initial reaction.[22] However, the oxidation of the Co(III) species was proposed to continue by reaction with another $Ru(bpy)_3^{3+}$ molecule to generate Co(IV) which could then react with water to produce H_2O_2. In the zeolite, the entrapped Ru(III) are surrounded by two types of cobalt(II) ions. The hydrated cobalt ions that are mobile in the zeolite cages $Co(H_2O)_6^{2+}$ should have similar reduction potentials as cobalt ions in aqueous solution (1.86 V)[23] and are not expected to react with the Ru(III) complexes. The second type of Co(II) ions will be coordinated to the zeolite oxygens and should have a different reduction potential. We propose that these ions are capable of participating in the electron transfer reactions with $Ru(bpy)_3^{3+}$. These are, however, bound to the zeolite cages and their mobility is restricted. Thus, it is not surprising that no evolution of O_2 is observed for the zeolite system since the formation of Co(IV) is improbable. The lack of any O_2 formation in this case suggests that the small amounts of transition metal impurities at the ppm levels in the zeolite are not causing the effects that we observe in this study.

(23) Wamiquist, B. *Inorg. Chem.* **1970**, *9*, 682.

Conclusions

$Ru(bpy)_3^{3+}$ trapped in the supercages of zeolite-Y will oxidize intrazeolitic water to dioxygen slowly, but with high efficiency. Zeolite entrapment eliminates the multimolecular degradation pathways typically observed in solution. The rate and degree of completion of this reaction is dependent on the internal acidity of the zeolite. Various intermediates were observed by diffuse reflectance, Raman, and EPR spectroscopies. The reaction is initiated by water attack on the bipyridyl ligand to form a covalent hydrate. Under basic conditions, deprotonation of this complex promotes the further reaction of $Ru(bpy)_3^{3+}$ with water. The slow step in the process is the loss of hydroxyl radical by homolytic fission of the C−OH bond. Evidence for the role of hydroxyl radical is provided by both its EPR spectra and spin trapping experiments. A base-mediated reaction is proposed for the formation of H_2O_2 from the hydroxyl adduct. The conversion of H_2O_2 to O_2 occurs by chemistry that is well-described in the literature. Experiments in the presence of Co^{2+} ion exchanged into the zeolite shows that a single-electron outer-sphere electron transfer occurs, but no oxygen evolution is observed. This also supports our contention that oxygen evolution is not being catalyzed by transition metal impurities present in the zeolite. This study illustrates that entrapment of molecules in zeolite cages allows the observation of chemistry that is not feasible under typical homogeneous conditions by eliminating pathways that involve multimolecular reaction steps.

Acknowledgment. We acknowledge the funding from the U.S. Department of Energy- Basic Science Program for funding this research. The assistance of Mr. David Chang in doing the mass spectrometry experiments is also appreciated.

Supporting Information Available: Plot of diffuse reflectance spectra of $Ru(bpy)_3^{2+}$ and $Ru(bpy)_3^{2+}$ in Zeolite Y and complete experimental details on materials and syntheses used in this research (5 pages). This material is contained in many libraries on microfiche, immediately follows this article in the microfilm version of the journal, can be ordered from the ACS, and can be downloaded from the Internet; see any current masthead page for ordering information and Internet access instructions.

JA9439837